A fast method for computing arbitrary order Stress-Intensity Factor derivatives of 3D finite element simulations using Hypercomplex Automatic Differentiation

Mauricio Aristizabal, PhD

Harry Millwater, Professor

Arturo Montoya, Professor

WCCM 2024/ PANACM 2024
Vancouver, BC, Canada
July 24, 2024

University of Texas at San Antonio

Analogy with the finite difference method

Finite Difference (FD)

Perturb along the real axis

$$\frac{df}{dx} \approx \frac{f(x+\hat{h}) - f(x)}{\hat{h}}$$

Subtraction errors occur when $h \to 0$

Complex Taylor Series Expansion (CTSE)

CTSE is performed analogously to FD

Perturb along the imaginary axis

$$\frac{df}{dx} \approx \frac{Im(f(x+ih))}{h}$$

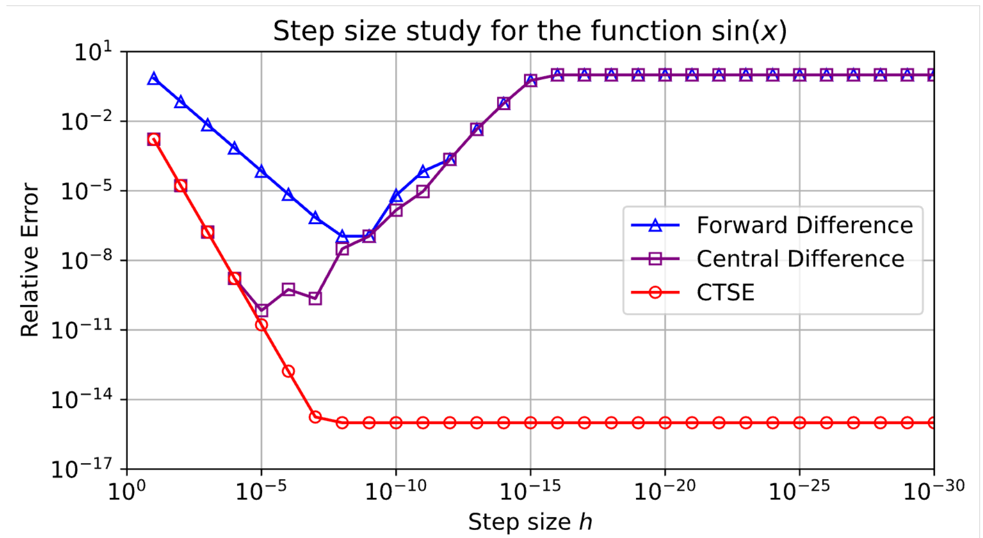

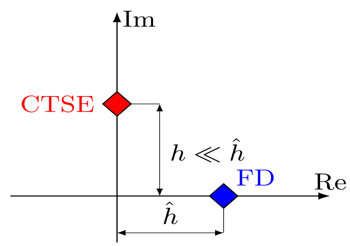

The step size can be made arbitrarily small with no concern about round-off error – **no subtraction error.**

Method – in a nutshell

- Uses hypercomplex algebra combined with traditional finite element methods to compute ***arbitrary order high accuracy derivatives***.
  - Step size independent method ensures high accuracy.
  - The traditional real-valued results are still obtained.

- Methodology programmed as a user element (UEL) within **Abaqus**.
  - Intrusive – code has to be reprogrammed for hypercomplex algebra but traditional functions still used, e.g., same shape functions, etc.

```
COMPLEX(KIND=r8),DIMENSION(MCRD  ,NNODE/2 ) :: zCOORDS
COMPLEX(KIND=r8),DIMENSION(NNODE,NNODE)::zAMATRX !Complex Stiffness Matrix
```

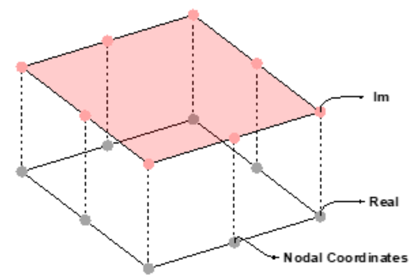

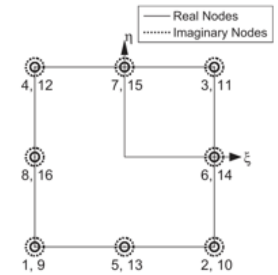

Perturbations

- Arbitrary *shape*, *material* and *loading* sensitivities are available.

- Perturb nodal coordinates in imaginary axis only!

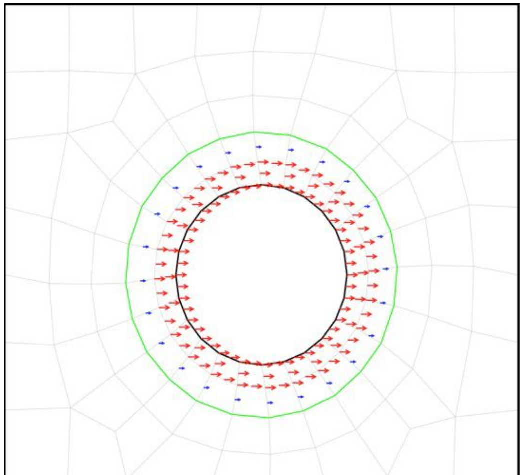

Horizontal Perturbation

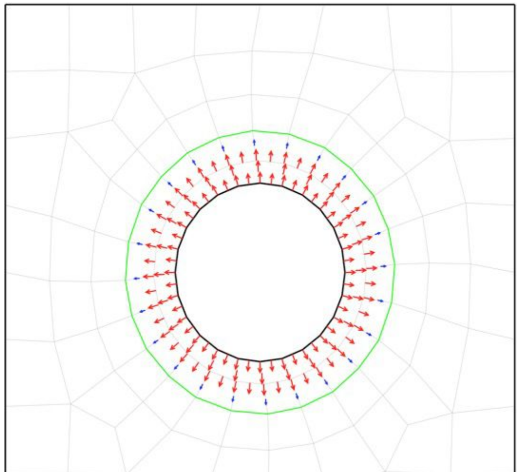

Radial Perturbation

Minimal mesh distortion issues!

Imaginary nodal coordinates define the ***perturbation*** in the shape.

Calculation of the Energy Release Rate

$G = \pm\frac{dU}{dA}$ - special case of shape sensitivity. Perturb the crack area along the imaginary axis and extract the imaginary component of strain energy:

$$G = \pm\frac{dU}{dA} \approx \frac{1}{\Delta A}\sum_{el=1}^{Nel} Im(U_{el})$$

ΔA is related to the step size h – typically 10^{-10} times the smallest element at the crack tip.

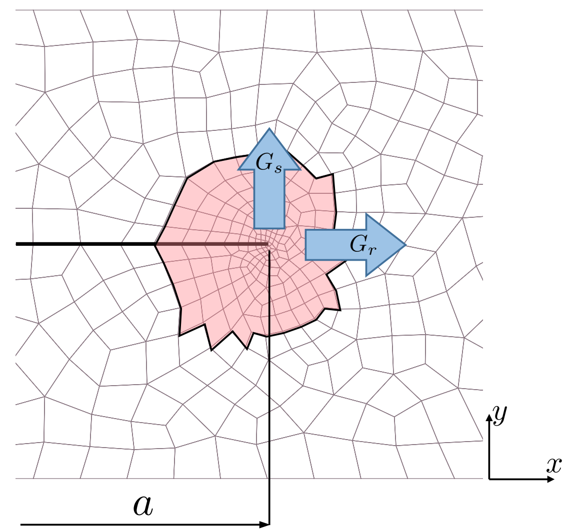

Mesa function **Pyramid function**

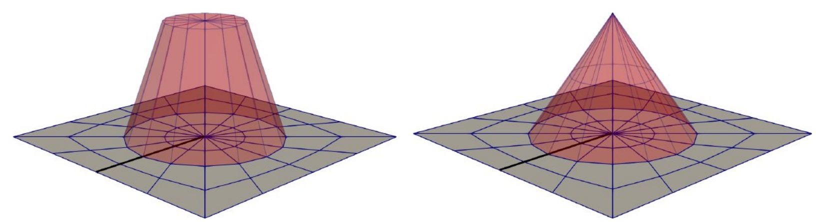

Bi-Material Fracture

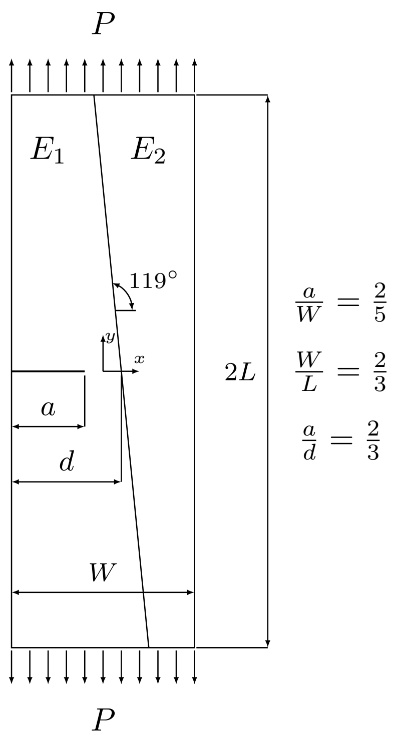

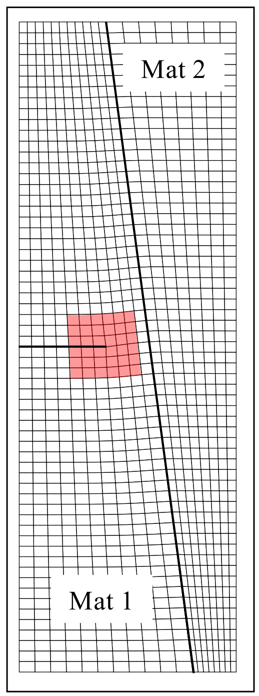

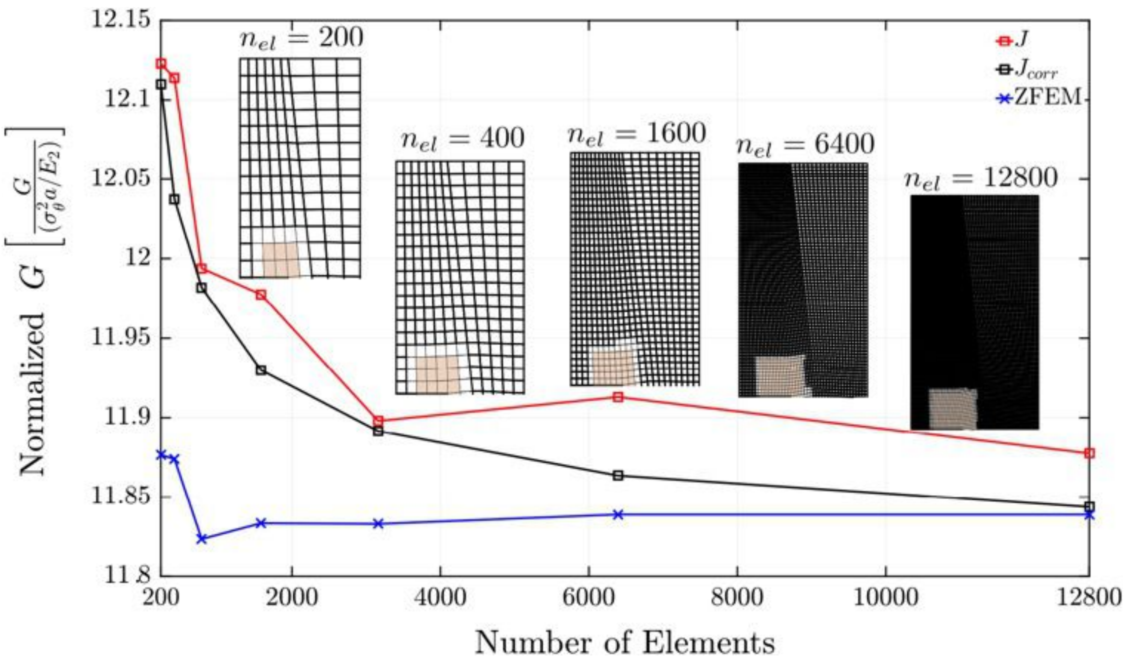

J-integral: $J = -\frac{d\Pi}{da} = \int_{\Gamma_0} \left(W n_1 - T_i \frac{\partial u_i}{\partial x_1} \right) ds$

University of Texas at San Antonio

Virtual crack extension method for thermoelastic fracture using a complex-variable FEM

Nodal Perturbations along crack face

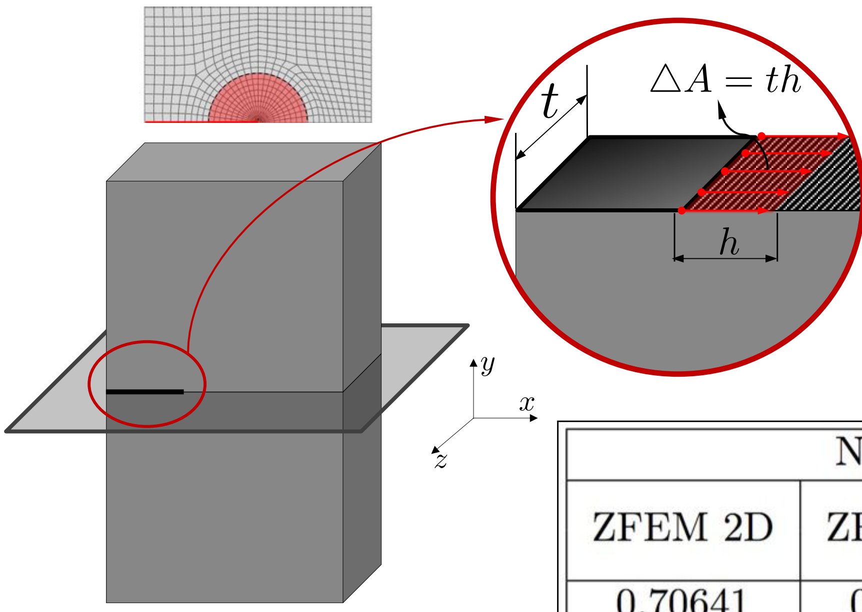

Energy Release Rate

$$G = -\frac{1}{\triangle A} Im[U^*]$$

Normalized G $\left[G/(\sigma_\theta^2 a/E)\right]$			
ZFEM 2D	ZFEM 3D	2D Abaqus 10^{th} Contour	3D Abaqus 10^{th} Contour
0.70641	0.70662	0.70640	0.70662

D. Ramirez Tamayo*, A. Montoya, H.R. Millwater, “A Virtual Crack Extension Method for Thermoelastic Fracture Using a Complex-Variable Finite Element Method”, Engineering Fracture Mechanics 192 (2018) 328-342, https://doi.org/10.1016/j.engfracmech.2017.12.013

A Complex-Variable Virtual Crack Extension FEM for Elastic-Plastic Fracture Mechanics

- Extends ZFEM for elastic-plastic materials.
- In contrast to J-integral, ZFEM achieves contour path independence, and **it is not restricted to monotonic loading**.

CT specimen under uncontained yielding conditions. Highlighted plastic regions correspond to line-load displacement of 0.4140 mm.

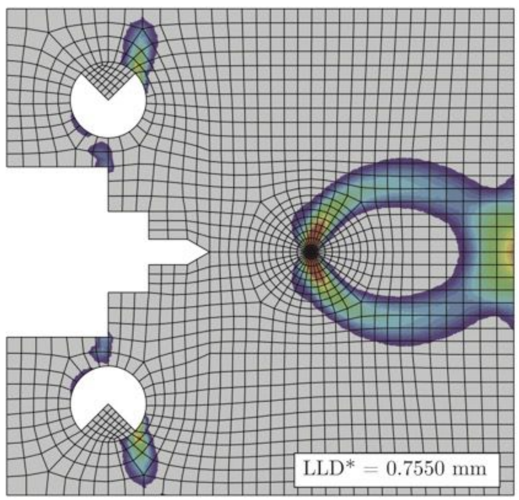

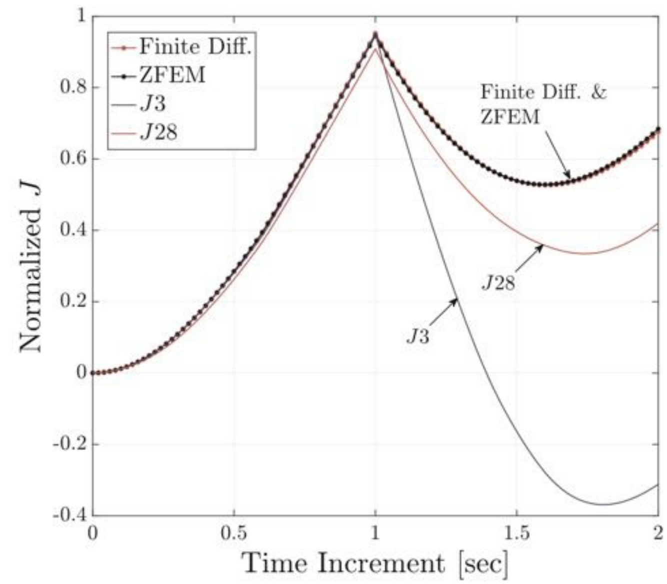

A. Montoya, D. Ramirez Tamayo*, H.R. Millwater, and M. Kirby*, "A Complex-Variable Virtual Crack Extension Finite Element Method for Elastic-Plastic Fracture Mechanics, Engineering Fracture Mechanics", 202 (2018) 242-258 https://doi.org/10.1016/j.engfracmech.2018.09.023

Hypercomplex Algebras

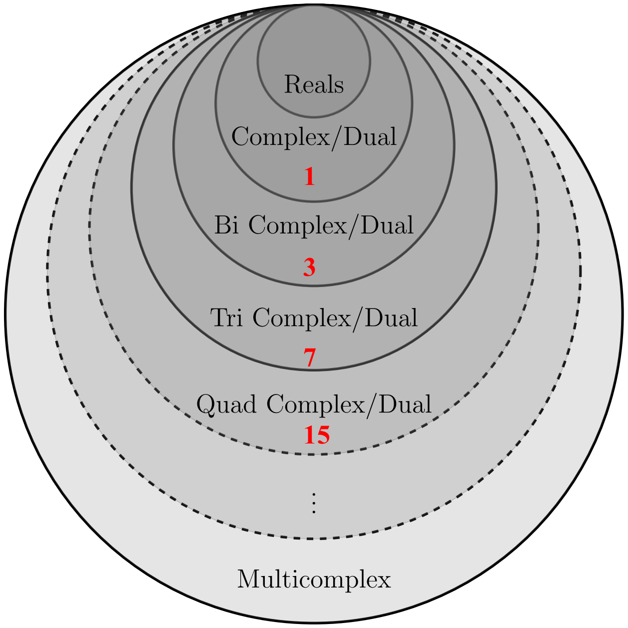

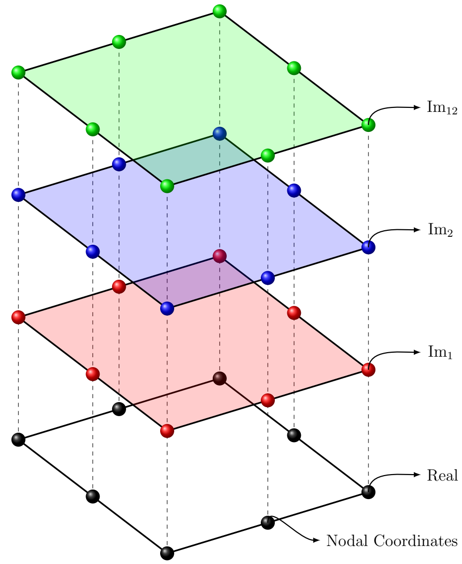

HYPAD Info

Multiple imaginary axes → multiple arbitrary order derivatives

Lantoine, G.; Russell, RP.; Dargent, T. (2012). Using Multicomplex Variables for Automatic Computation of High-order Derivatives. *ACM Transactions on Mathematical Software, 38*(3), 21.
Fike, J. & Alonso, J. The Development of Hyper-Dual Numbers for Exact Second-Derivative Calculations. in 49th AIAA Aerospace Sciences Meeting including the New Horizons Forum and Aerospace Exposition (AIAA, 2011). doi:10.2514/6.2011-886

Non-intrusive Residual Method

- Residual Concept:

$$\mathbf{r}(\mathbf{u}(a), a) = \mathbf{0} \qquad \frac{d^n \mathbf{r}}{d a^n} = \mathbf{0}$$

- In Linear elasticity, $\mathbf{r}(\mathbf{u}, a) = \mathbf{K}\mathbf{u} - \mathbf{f} = 0$

$$\mathbf{K}\frac{\partial \mathbf{u}}{\partial a} = \frac{\partial \boldsymbol{r}}{\partial a} = \frac{\partial \mathbf{f}}{\partial a} - \frac{\partial \mathbf{K}}{\partial a}\mathbf{u}$$

RHS difficult to obtain in closed form

$$\mathbf{K}\frac{\partial^2 \mathbf{u}}{\partial a^2} = \frac{\partial^2 \boldsymbol{r}}{\partial a^2} = \frac{\partial^2 \mathbf{f}}{\partial a^2} - 2\frac{\partial \mathbf{K}}{\partial a}\frac{\partial \mathbf{u}}{\partial a} - \frac{\partial^2 \mathbf{K}}{\partial a^2}\mathbf{u}$$

- New **residual approach**:

$$\mathbf{K}\frac{\partial \mathbf{u}}{\partial a} = -\mathrm{Im}_{\epsilon_1}[\mathbf{r}(\mathbf{u}, a + \epsilon_1)]$$

$$\mathbf{K}\frac{\partial^2 \mathbf{u}}{\partial a^2} = -\mathrm{Im}_{\epsilon_1^2}\left[\mathbf{r}\left(\mathbf{u} + \frac{\partial \mathbf{u}}{\partial a}\epsilon_1, a + \epsilon_1\right)\right]$$

RHS obtained automatically from HYPAD

Advantages

- Non-intrusive postprocessing approach.
- Applicable to transient linear and non-linear problems.
- Parallelizable and memory efficient.
- Does not compute derivatives of tangent-stiffness matrix (which are costly)

Non-intrusive Residual Method

- Generalized form:

$$\mathbf{r}(\mathbf{u}, a) = \mathbf{K}(\mathbf{u})\mathbf{u} - \mathbf{f} = 0$$

- First order derivatives:

$$\mathbf{T}\frac{\partial \mathbf{u}}{\partial a} = -\mathrm{Im}_{\epsilon_1}[\mathbf{r}(\mathbf{u}, a + \epsilon_1)]$$

- Second order derivatives:

$$\mathbf{T}\frac{\partial^2 \mathbf{u}}{\partial a^2} = -\mathrm{Im}_{\epsilon_1^2}\left[\mathbf{r}\left(\mathbf{u} + \frac{\partial \mathbf{u}}{\partial a}\epsilon_1, a + \epsilon_1\right)\right]$$

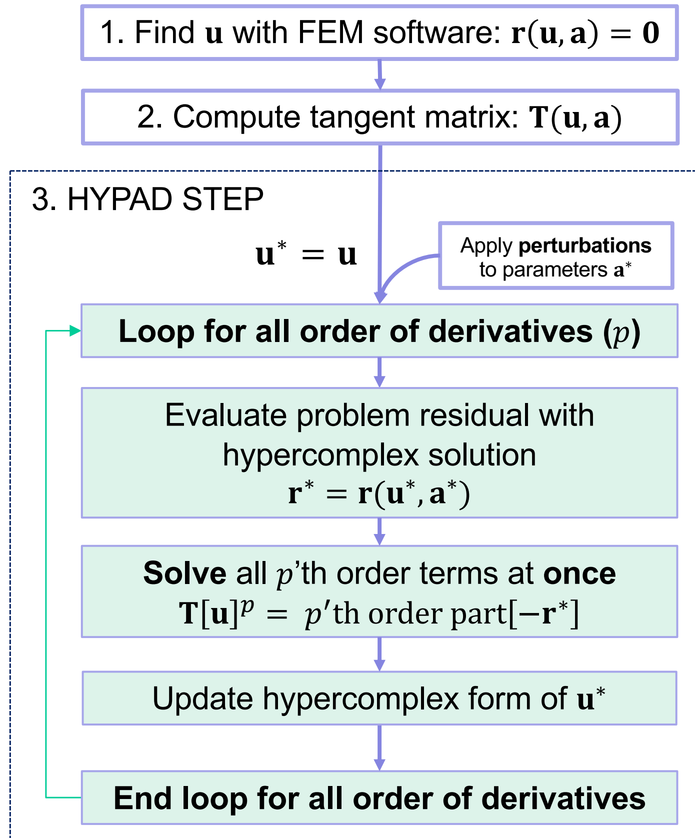

Efficient 3D ERR and Mode-I SIF sensitivities

- Analyzed a 3D penny-shaped crack problem with FEM (20 node bricks) to compute ERR and SIF.
- Displacements obtained using Abaqus.
- Methods: 1) **HYPAD + VCE** and 2) **HYPAD + J-integral**.
- Computed up to **3rd order** derivatives of ERR and SIF to a, E, ν and σ **(34 derivatives) with residual method.**

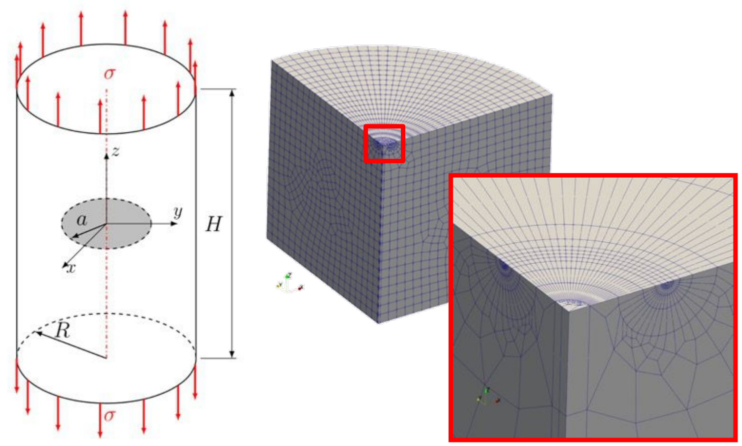

Mesh Statistics	Elements	Nodes	Total DOFs
Fine mesh	175 098	718 376	2 155 128

University of Texas at San Antonio

Analytical solution of 3D Penny-shaped crack

- Analytic solution of ERR for Penny-shaped crack.

$$\boldsymbol{G} = \frac{K_I^2}{\frac{E}{1-\nu^2}} = 4(1-\nu^2)\frac{\sigma^2 a}{\pi E}$$

- ERR has 27 Non-zero derivatives

- Results **HYPAD + J-Integral**:
  - ZFEM + residual → compute derivatives of u
  - ERR obtained with hypercomplex

Derivative	Relative Error [%]
$\boldsymbol{G}$	0.016
$\partial\boldsymbol{G}/\partial a$	0.048
$\partial\boldsymbol{G}/\partial E$	0.016
$\partial\boldsymbol{G}/\partial \nu$	0.017
$\partial\boldsymbol{G}/\partial \sigma$	0.016
$\partial^2\boldsymbol{G}/\partial a^2$	--------
$\partial^2\boldsymbol{G}/\partial a\partial E$	0.048
$\partial^2\boldsymbol{G}/\partial E^2$	0.016
$\partial^2\boldsymbol{G}/\partial a\partial \nu$	0.341
$\partial^2\boldsymbol{G}/\partial E\partial \nu$	0.017
$\partial^2\boldsymbol{G}/\partial \nu^2$	0.087
$\partial^2\boldsymbol{G}/\partial a\partial \sigma$	0.048
$\partial^2\boldsymbol{G}/\partial E\partial \sigma$	0.016
$\partial^2\boldsymbol{G}/\partial \nu\partial \sigma$	0.017
$\partial^2\boldsymbol{G}/\partial \sigma^2$	0.016

Derivative	Relative Error [%]
$\partial^3\boldsymbol{G}/\partial a^3$	----------
$\partial^3\boldsymbol{G}/\partial a^2\partial E$	----------
$\partial^3\boldsymbol{G}/\partial a\partial E^2$	0.048
$\partial^3\boldsymbol{G}/\partial E^3$	0.016
$\partial^3\boldsymbol{G}/\partial a^2\partial \nu$	----------
$\partial^3\boldsymbol{G}/\partial a\partial E\partial \nu$	0.341
$\partial^3\boldsymbol{G}/\partial E^2\partial \nu$	0.017
$\partial^3\boldsymbol{G}/\partial a\partial \nu^2$	0.728
$\partial^3\boldsymbol{G}/\partial E\partial \nu^2$	0.087
$\partial^3\boldsymbol{G}/\partial \nu^3$	----------
$\partial^3\boldsymbol{G}/\partial a^2\partial \sigma$	----------
$\partial^3\boldsymbol{G}/\partial a\partial E\partial \sigma$	0.048
$\partial^3\boldsymbol{G}/\partial E^2\partial \sigma$	0.016
$\partial^3\boldsymbol{G}/\partial a\partial \nu\partial \sigma$	0.341
$\partial^3\boldsymbol{G}/\partial E\partial \nu\partial \sigma$	0.017
$\partial^3\boldsymbol{G}/\partial \nu^2\partial \sigma$	0.087
$\partial^3\boldsymbol{G}/\partial a\partial \sigma^2$	0.048
$\partial^3\boldsymbol{G}/\partial E\partial \sigma^2$	0.016
$\partial^3\boldsymbol{G}/\partial \nu\partial \sigma^2$	0.017
$\partial^3\boldsymbol{G}/\partial \sigma^3$	----------

3D Penny-shaped crack – ERR Sensitivities

- **ERR** analytic solution for Penny-shaped crack.

$$G = 4(1-\nu^2)\frac{\sigma^2 a}{\pi E}$$

- All derivatives below **1%** relative error

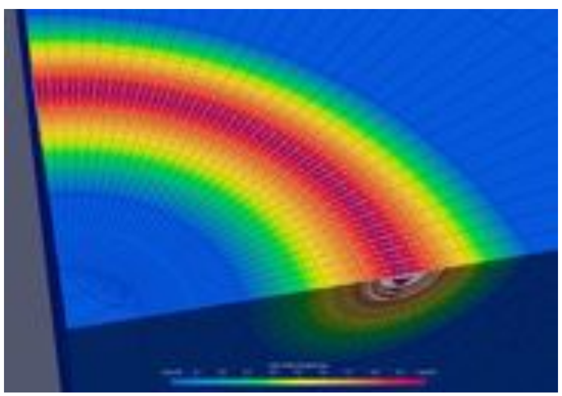

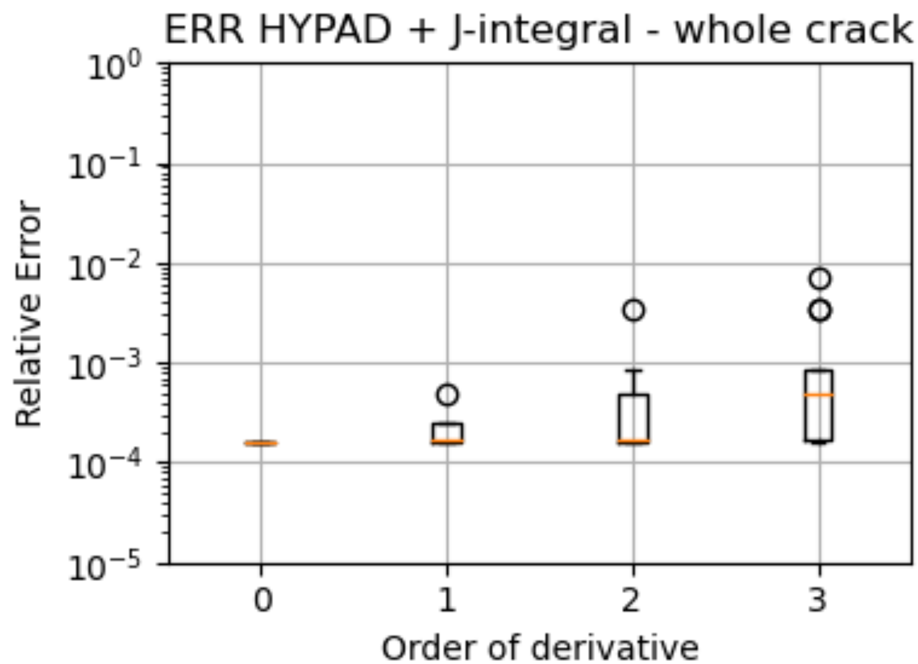

34 derivs (4 first, 10 second and 20 third)

3D Penny Shaped crack – Performance results

- Implementation: Fortran + Python code run in a node with
  - 2x Intel(R) Xeon(R) Gold 6248 CPU (up to 40 cores)
  - 376 GB RAM

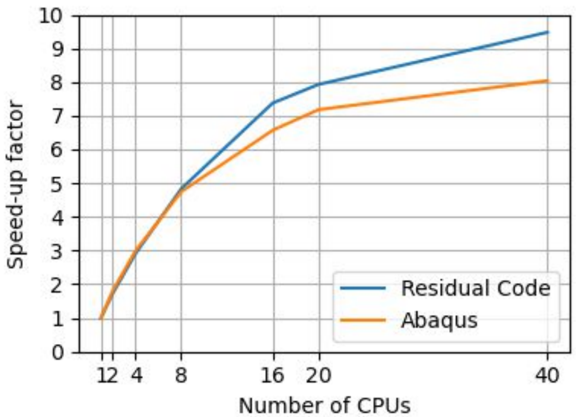

- Residual method approximately **~2X** Abaqus real run

- Residual method scales well with parallelization.

- Each order of derivative adds around 7% CPU time.

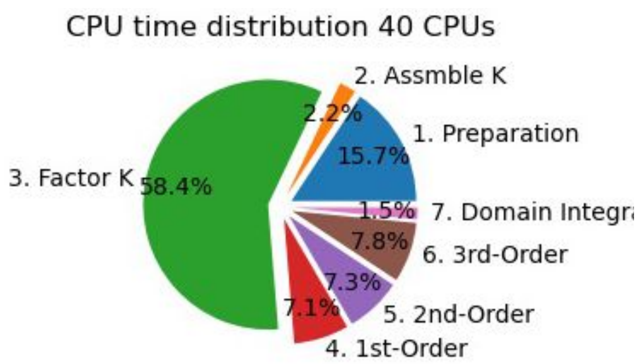

Interaction integral (Overview)

- Also known as **M-integral**- calculates the mutual energy release rate

$$M = \int_A \left(\sigma_{ij}^{\text{aux}} u_{j,1} q_{,i} + \sigma_{ij} u_{j,1}^{\text{aux}} - \sigma_{jk}^{\text{aux}} \varepsilon_{jk} q_{,1} \right) \mathrm{d}A,$$

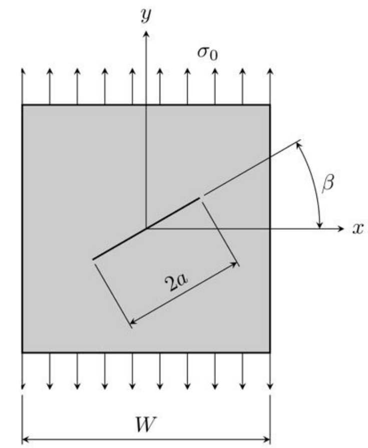

- Used in the calculation of **mixed-mode stress intensity factors**.

$$M(u_{j,1}, u_{j,1}^{\text{aux}}, \sigma_{ij}^{\text{aux}}) = \begin{cases} M_I & \text{if } K_I^{\text{aux}} = 1 \text{ and } K_{II}^{\text{aux}} = 0, \\ M_{II} & \text{if } K_I^{\text{aux}} = 0 \text{ and } K_{II}^{\text{aux}} = 1. \end{cases}$$

$$K_I = \frac{E'}{2} M_I, \quad K_{II} = \frac{E'}{2} M_{II}, \qquad \text{where } E' = \begin{cases} E & \text{for plane stress,} \\ E/(1-\nu^2) & \text{for plane strain.} \end{cases}$$

UTSA®

University of Texas at San Antonio

2D mixed-mode stress intensity factor rates using a complex-variable interaction integral - dK/da

- Applies ZFEM to the **interaction integral**.

$$M_e^* = \int \Big[\underbrace{\sigma_{ij}^{*\,\text{aux}}}_{\text{CTSE}} \underbrace{u_{j,1}^{*}}_{\text{ZFEM}} \underbrace{q_{,i}^{*}}_{\text{CTSE}} + \underbrace{\sigma_{ij}^{*}}_{\text{ZFEM}} \underbrace{u_{j,1}^{*\,\text{aux}}}_{\text{CTSE}} \underbrace{q_{,i}^{*}}_{\text{CTSE}} - \underbrace{\sigma_{jk}^{*\,\text{aux}}}_{\text{CTSE}} \underbrace{\varepsilon_{jk}^{*}}_{\text{ZFEM}} \underbrace{q_{,1}^{*}}_{\text{CTSE}} \Big] \underbrace{|\mathbf{J}^*|}_{\text{CTSE}} \, \mathrm{d}\xi \mathrm{d}\eta, \qquad M^* = \sum_{\Omega_e \subset \Omega_M} M_e^*,$$

$$\frac{\partial K_I}{\partial a} = \frac{E'}{2} \frac{\mathrm{Im}\left(M_I^*\right)}{h}$$

$$\frac{\partial K_{II}}{\partial a} = \frac{E'}{2} \frac{\mathrm{Im}\left(M_{II}^*\right)}{h}$$

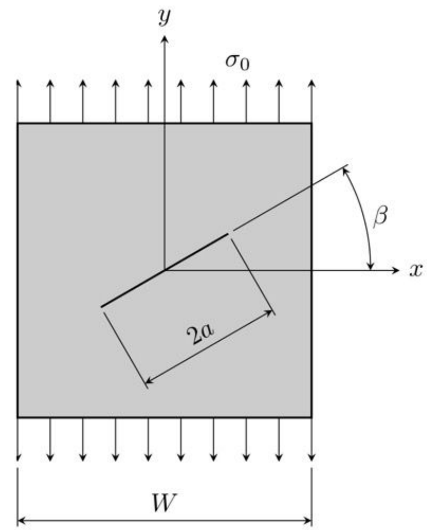

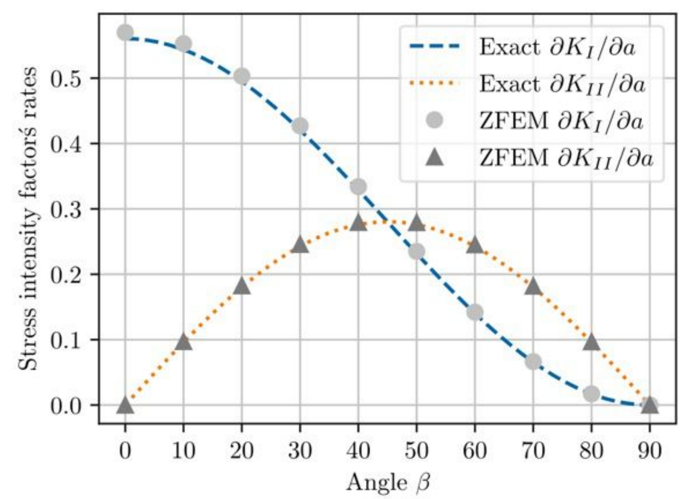

A. Aguirre-Mesa*, S. Restrepo-Velasquez*, D. Ramirez-Tamayo, A. Montoya and H. Millwater, "Computation of two dimensional mixed-mode stress intensity factor rates using a complex-variable interaction integral," 277 (2023) Engineering Fracture Mechanics, https://doi.org/10.1016/j.engfracmech.2022.108981

Inclined Penny-Shaped Crack problem

- Parameters for the analysis were as follows*:

Parameter		Value
Crack Inclination	γ	45°
Crack length	r	0.125
Dimension	l_x, l_z	5.0
	l_y	10.0

Parameter		Value
Young modulus	E	10 000
Poisson's ratio	ν	0.0
Far-field stress	σ	1.0

*Corresponds to benchmark problem 3 in Franc3D website.

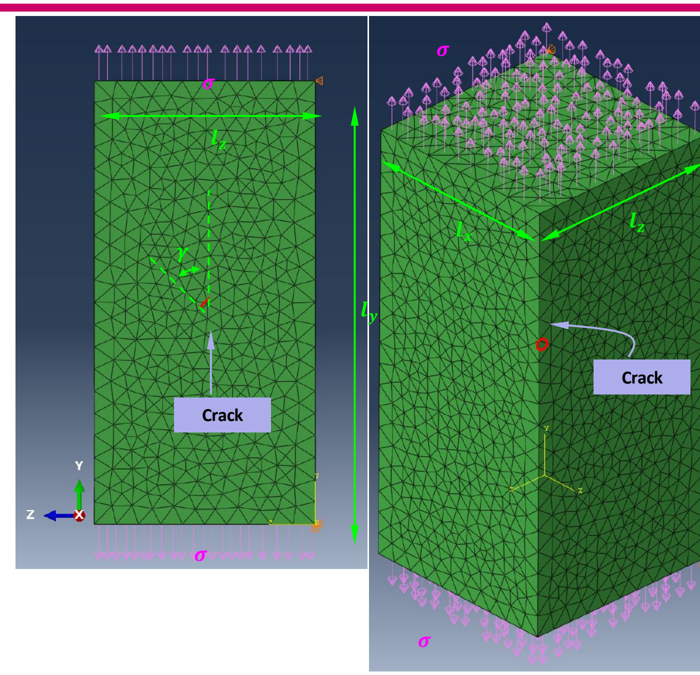

- SIFs analytical solution (Murakami, 1987)

$$K_I = \frac{2\sigma}{\pi}\sqrt{\pi r}\,\sin^2(\gamma)$$

$$K_{II} = \frac{2\sigma}{\pi}\sqrt{\pi r}\,\sin(\gamma)\cos(\gamma)\sin(\theta)\,\frac{2}{2-\nu}$$

$$K_{III} = \frac{2\sigma}{\pi}\sqrt{\pi r}\,\sin(\gamma)\cos(\gamma)\cos(\theta)\frac{2(1-\nu)}{2-\nu}$$

Mesh Statistics	Wedge 15	Brick 20	Tetra 10	Total Elements	Nodes	Total DOFs
Value	2 360	14 160	111 374	**127 894**	**228 814**	**646 442**

Inclined Penny-Shaped Crack problem – Results

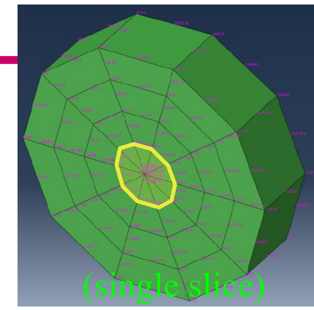

Results for **ring 0** of elements – vertex perturbation (two slices).

- This ring contains only wedge15, two element slices.
- Computed using q-function for wedge vertex nodes.
  - Q-function linear in element, two slice span.
- Results show error of 0.284% to analytical solution.

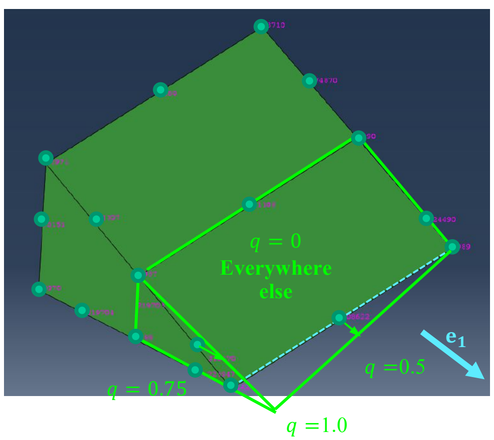

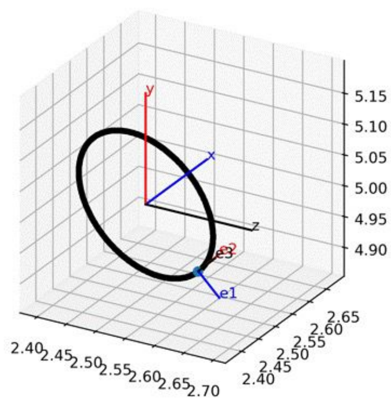

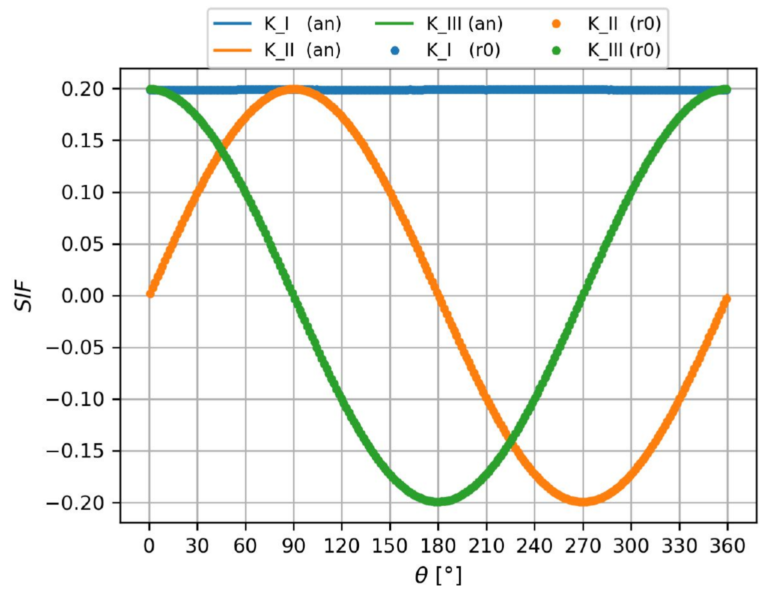

Inclined Penny-Shaped Crack problem – Results

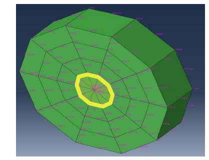

First order derivatives

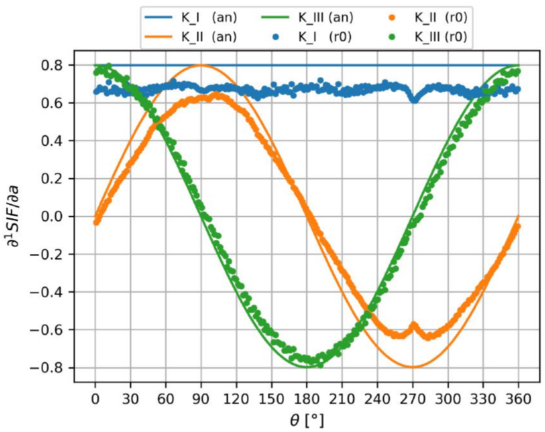

a

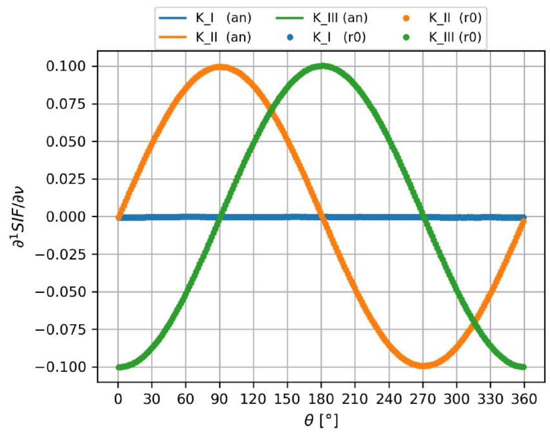

v

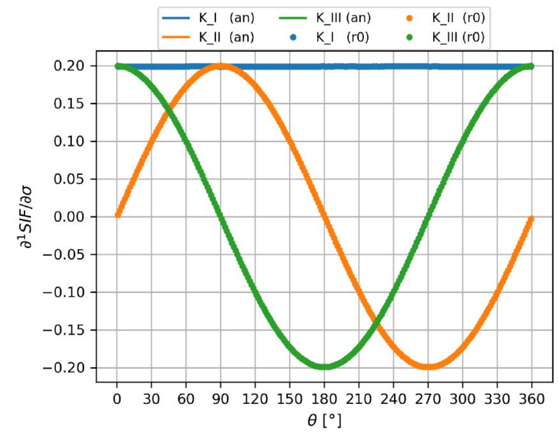

σ

UTSA

University of Texas at San Antonio

Inclined Penny-Shaped Crack problem – Results

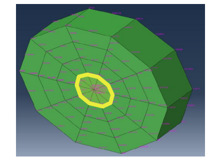

Second order derivatives

a,v

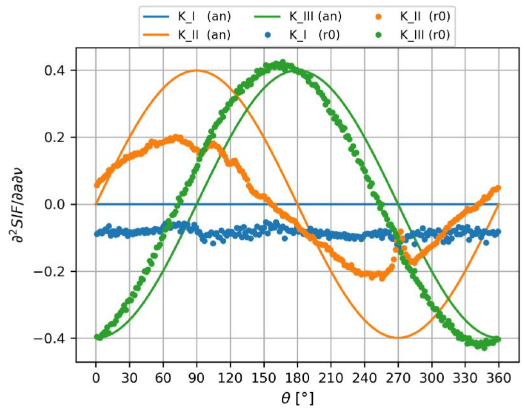

a,σ

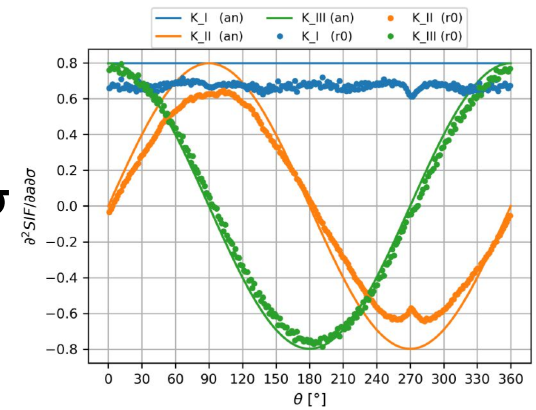

v

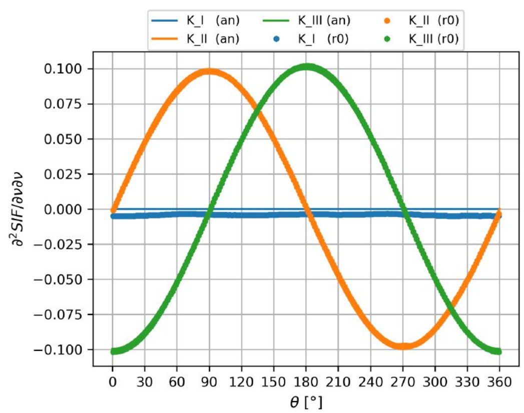

v,σ

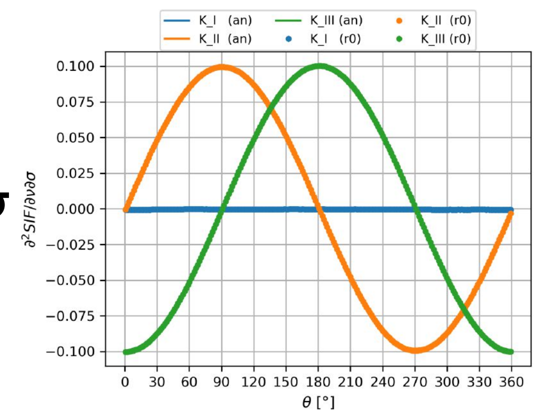

Inclined Penny-Shaped Crack problem – Results

Third order derivatives

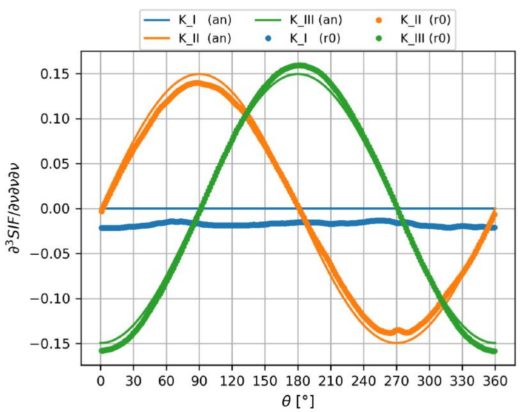

v

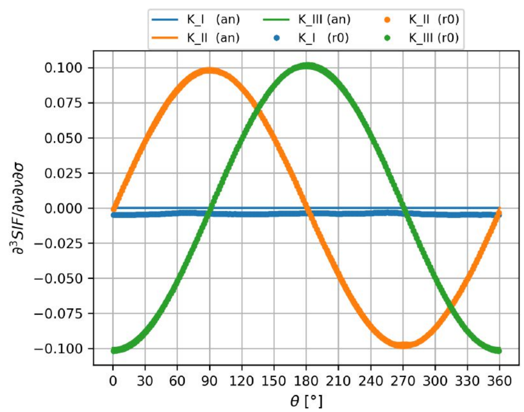

v, σ

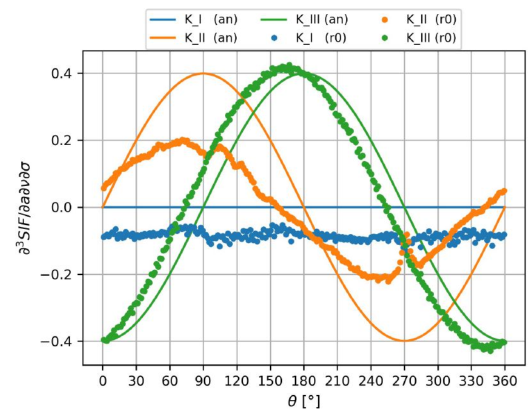

a,v,σ

University of Texas at San Antonio

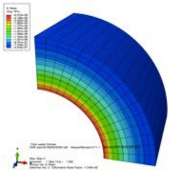

Summary

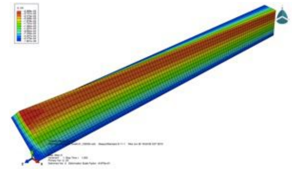

- Elegant, straightforward method to compute G, K, and its derivatives with respect to crack size and any other parameter.
  - Promote variables to complex/hypercomplex.
  - Largely use the same/existing solution methods.

- Higher order derivatives are available.
  - Applicable to linear and nonlinear problems.

- ***Non-intrusive residual method very effective for 3D fracture.***
  - Residual method approximately **~2X** Abaqus real run

Acknowledgements

- Efficient Sensitivity Methods for Probabilistic Lifing and Engine Prognostics, Pat Golden, AFRL/RXLMN, Aug. 2007-Sep. 2010
- Efficient Finite Element-based 3D Fracture Mechanics Crack Growth Analysis using Complex Variable Sensitivity Methods, DoD PETTT, Sep. 2010 - Aug. 2011
- Implementation of Complex Variable Finite Element Methods in Abaqus, DOD PETTT, Sep. 2011- Aug. 2012
- Enhanced Fracture Mechanics Crack Growth Analysis using Complex Variable Sensitivity Methods, AFOSR (David Stargel), May 2011-2014
- Probabilistic Residual Stress Modeling, AFRL through Clarkson Aerospace, Sept. 2012 – Dec. 2018
- A New Progressive Curvilinear Strain Energy-based Crack Growth Modeling Algorithm using Multicomplex Variable Finite Elements, Bill Nickerson, ONR, Sept. 2013-Sept. 2016
- Three Dimensional Fracture Mechanics Capability for Structures operating in High Temperature Thermal Environments, DoD, Aug. 2015-Aug. 2018.
- A Fast and Effective Sensitivity and Uncertainty Quantification Method for Additively Manufactured Metals, Aug. 2020 – July 2024, Michael Bakas, Army Research Office (ARO) grant W911NF2010315
- 3D Fracture Simulations using the Hypercomplex Finite Element Software, July 2020 – Feb. 2024, Metis Design Corporation – Alan Timmons, NavAir SBIR Program (SBIR Phase II.5 N12-T007), Contract No. N68335-20-C-0858